Drug Design, Development and Therapy

Dovepress
Taylor & Francis Group

Open Access Full Text Article

ORIGINAL RESEARCH

ITGA4 Contributes to 5-Fluorouracil Resistance by Up-Regulating PI3K/AKT Signaling: Evidence from Network Pharmacology, Molecular Docking and Experimental Verification

Sicheng Yan[1], Xiaomeng Hu[1], Yan Wu[1], Wangfang Ye[1], Yuehong Zhu[1], Yuxuan He[1], Fuyuan Zhan[1,2], Wei Wu[3], Zhihong Ma[1,2]

[1]Huzhou Key Laboratory of Molecular Medicine, Huzhou Central Hospital, Fifth School of Clinical Medicine of Zhejiang Chinese Medical University, Huzhou, Zhejiang, 313000, People's Republic of China; [2]School of Basic Medicine College, Zhejiang Chinese Medical University, Hangzhou, Zhejiang, 310000, People's Republic of China; [3]Key Laboratory of Multiomics Research and Clinical Transformation of Digestive Cancer of Huzhou, Huzhou Central Hospital, Fifth School of Clinical Medicine of Zhejiang Chinese Medical University, Huzhou, Zhejiang, 313000, People's Republic of China

Correspondence: Wei Wu, Key Laboratory of Multiomics Research and Clinical Transformation of Digestive Cancer of Huzhou, Huzhou Central Hospital, Fifth School of Clinical Medicine of Zhejiang Chinese Medical University, Huzhou, Zhejiang, 313000, People's Republic of China, Tel +86 05722023301, Email hchwuwei2018@126.com; Zhihong Ma, Huzhou Key Laboratory of Molecular Medicine, Huzhou Central Hospital, Fifth School of Clinical Medicine of Zhejiang Chinese Medical University, Huzhou, Zhejiang, 313000, People's Republic of China, Tel +86-187572951 86, Email mazhihong@hzhospital.com

Objective: 5-Fluorouracil (5-FU) is a mainstream drug used in chemotherapy and chemoradiotherapy regimens for the clinical treatment of malignancies, such as gastric cancer (GC), colorectal cancer, and breast cancer. However, the molecular mechanism of action of 5-FU in GC has not yet been studied using a network pharmacology approach.

Methods: The mechanism of action of 5-FU in GC was determined using a network pharmacology technique, and our findings were confirmed by various computational approaches and experimental tests using the GeneCards database, ChEMBL database, STRING database, molecular docking, molecular dynamics simulation, DAVID, GEPIA, Kaplan–Meier Plotter, CCK-8 assays, colony formation experiments, cell proliferative assay, apoptosis assays, wound-healing assays, Real-time PCR and Western blot tests.

Results: A total of 21 shared and 13 potential targets were identified using PPI network analysis. Kyoto Encyclopaedia of Genes and Genomes (KEGG) enrichment analyses indicated that the PI3K/AKT signaling pathway may be a significant pathway. Combined with molecular docking and database verification, F10, NR3C1, DHFR, CA2, BCHE, ACHE, and ITGA4 were identified as candidate core genes. Moreover, the experimental results illustrated that ITGA4 induces 5-FU resistance by up-regulating PI3K/AKT signaling.

Conclusion: Network pharmacology is a feasible scientific research strategy for revealing the multitarget-multipathway role of 5-FU in the treatment of GC and provides ITGA4-based new ideas and therapeutic strategy to overcome 5-FU resistance for GC treatment.

Keywords: 5-FU, gastric cancer, network pharmacology, molecular docking, ITGA4, PI3K/AKT pathway, resistance

Introduction

Gastric cancer (GC) is the fifth most common malignant tumor worldwide and has a poor prognosis. In 2020, there were an estimated 19.3 million new cancer cases worldwide; GC accounted for 5.6% of cancer cases and 7.7% of cancer-related deaths.[1] The diagnosis rate of GC is unsatisfactory owing to its insidious onset, and most new patients have advanced GC at diagnosis. Despite advances have been made in surgical techniques, radiotherapy, chemotherapy, and neoadjuvant therapy, the prognosis of patients with metastasis or recurrence remains poor, and GC remains a lethal disease worldwide.[2] Therefore, the exploration of related therapeutic drugs is a hot topic in current research. The development and application of targeted therapies provide more choices for this field. 5-Fluorouracil (5-FU), also known as fluorouracil, is a pyrimidine analog. It is mainly used to treat tumors and has certain curative effects on digestive tract, breast, ovarian, choriocarcinoma, cervical, liver, bladder, and skin cancers.[3] It is used alone or in combination with other

Received: 28 August 2024
Accepted: 13 May 2025
Published: 20 May 2025

drugs in the adjuvant treatment of breast cancer and gastrointestinal cancer surgery, and for palliative treatment of some nonsurgical malignant tumors.[4] The clinical benefits of 5-FU treatment are often transient, and most patients do not achieve complete eradication of tumor cells, resulting in recurrence after 5-FU treatment and poor prognosis.[5] Therefore, strategies to improve the clinical outcomes of 5-FU treatment are urgently needed. Understanding the mechanism of action of 5-FU in GC treatment is important to improve its survival benefit.

Diseases, including GC, rarely arise from the imbalance of a solitary protein; rather, they generally manifest as alterations within intricate cellular networks. From a pharmacological standpoint, focusing on a singular disease-associated protein might not constitute an efficacious strategy and could potentially be misleading. Consequently, network pharmacology approaches have been suggested to address the limitations inherent in traditional targeted therapeutic strategies. Network pharmacology integrates systems network analysis with pharmacology to elucidate the molecular mechanisms of multi-target drugs by examining the "disease-gene-target-drug" interaction network, thereby emerging as a promising and comprehensive research approach. However, the mechanism of 5-FU, a synthetic drug, in treating GC has not yet been studied using this method. In this study, the target gene ITGA4 was identified through network pharmacology, and further research was conducted on its synergistic effect with 5-FU. Additionally, the function of the target gene ITGA4 was validated. Interestingly, ITGA4 was upregulated in cells after 5-FU treatment, and the upregulation of ITGA4 had a protective effect on the cells, showing stronger anti-apoptotic ability and higher drug resistance. These findings provide new insights into the development of ITGA4 inhibitors for the treatment of drug-resistant GC.

Materials and Methods

Network Pharmacology Analysis

The human gene disease-related database GeneCards (https://www.genecards.org/) provides all known and predicted human genes in the genome, proteome, transcription, genetics, and function. "Gastric cancer" was input into the GeneCards database to obtain GC-related genes.[6] The ChEMBL database (https://www.ebi.ac.uk/chembl/) is a large open-access drug discovery database designed to collect medicinal chemistry data and knowledge during drug research and development, including therapeutic targets and indications for clinical experimental drugs and approved drugs.[7] Information such as compound targets can be queried. "5-Fluorouracil" was used as an input to obtain the relevant targets, and the UniProt database (https://www.uniprot.org/) was converted to the corresponding gene name to screen the human gene ("Homo sapiens"). The drug active ingredient-related targets and disease targets were matched and mapped, and a Venn diagram was drawn by Venny 2.1 software to obtain the cross-targets of 5-FU and GC.

The STRING database (https://cn.string-db.org/) is a protein interaction database that can be used to search for interactions between known proteins, and targets corresponding to the active components and common targets related to cancer can be input into the STRING database.[8] The study species for this analysis were selected as humans ("Homo sapiens"), PPI with minimum required interaction scores > 0.4 were selected, free points were hidden, and PPI graphics were downloaded and saved. tsv format. Finally, Cytoscape was used for analysis, and core targets were predicted by "cytohubba" analysis.

Gene Ontology (GO) enrichment, including biological process (BP), cellular component (CC), and molecular function (MF), can be used to further analyze the role of target proteins in gene function and roughly understand the enrichment of differential genes. Kyoto Encyclopedia of Genes and Genomes (KEGG) pathway enrichment analysis can be used to understand the metabolic pathways that are significantly altered under experimental conditions, based on differentially expressed genes. Core target gene analysis of GO enrichment and KEGG pathway enrichment was performed using Sangerbox (http://www.sangerbox.com/tool). Statistical significance was defined as a P value of less than 0.05.

Molecular Docking

5-FU and the cross-targets obtained were subjected to molecular docking verification. The 3D structure of 5-FU was queried using the PubChem database (https://pubchem.ncbi.nlm.nih.gov/). The 3D structure of the selected target was downloaded from the Protein Data Bank (PDB) database (https://www.rcsb.org/) and the protein were treated with PyMOL (Version 2.5.1) software to remove water and ligands. At the same time, AutoDock Tools software was used for

hydrogenation and charge addition, and then Autodock software was used for docking to find the best docking site. Currently, there is no clear standard for the selection of active ingredient targets. It is generally believed that there is a possibility of spontaneous binding when the binding energy is less than 0. The lower the binding energy, the greater the binding possibility. When the binding energy is greater than zero, external forces may be required to promote binding. Finally, the optimal conformation was imported into PyMOL for visualization.

Bioinformatics Analysis

Core targets were analyzed using the online tool GEPIA (http://gepia.cancer-pku.cn/index.html) to confirm their mRNA expression levels and pathological stages in TCGA-STAD. Survival information for patients with upregulated or down-regulated core targets was assessed using the Kaplan-Meier Plotter (http://kmplot.com/analysis/) to evaluate prognosis.

Molecular Dynamics Simulation (MDS)

MDS is a molecular simulation method that has rapidly developed in recent years. Numerical methods are used to solve the motion equations of molecular systems based on classical, quantum, and statistical mechanics to simulate the structure and properties of molecular systems.[9] This is the third scientific research method reported to study the structure and properties of molecular systems after experimental and theoretical research methods. It is a powerful tool for studying the dynamic behavior of biological macromolecules, such as proteins and DNA, and is a powerful supplement to theoretical calculations and experiments. It can provide information on scientific issues such as the mechanism of action of biological molecules in physiological functions and the identification of small molecules and potential targets by simulating the movement of biological macromolecules in three-dimensional space.[10–13] The molecular dynamics software GROMACS 2021.6 was used to simulate the NR3C1-5-FU complex and ITGA4-5-FU complex as follows:[14] Multiwfn was used to calculate the RESP2 charge of the complex small molecule, the topology file was generated under the GAFF force field, and the corresponding parameterization file for the protein was generated in the AMBER14 SB force field.[15] Then, SPC/E water model molecules were added to the complex as the centre to generate a cubic water box, and the corresponding ions were added to the complex water box to maintain the electrical neutrality of the simulation system (NR3C1-5-FU added 6 Cl ions, ITGA4-5-FU added 19 Cl ions). After the system was completed, the conjugate gradient method was used to minimize the energy of the 500 steps to ensure that the system was fully stable A regular ensemble (NVT) was used, and the Berendsen hot bath method was used to control the temperature at 298.15 K; 50000 steps were simulated, and the step size was 2 fs. Then, the isothermal isobaric ensemble (NPT) was simulated with Parrinello-Rahman pressure control, an atmospheric pressure of 1, 50000 steps and a step size of 2 fs. Then, mdrun was performed with a step length of 2 fs, 250,00000 simulation steps, and a total simulation time of 50 ns, and the data were obtained for the corresponding analysis and mapping steps.

Chemical Reagents

5-FU was purchased from Shanxi Gloria Comercio Internacional Co., Ltd and pan-AKT kinase inhibitor capivasertib (CAP) was purchased from MedChemExpress.

Cell Culture

Human gastric adenocarcinoma AGS, MKN45, and MGC803 cells were purchased from American Type Culture Collection (ATCC, Manassas, VA, United States). Cells were maintained in RPMI 1640 (Gibco) supplemented with 10% fetal bovine serum (FBS) and 1% penicillin/streptomycin (Gibco) at 37 °C under a humidified atmosphere containing 5% CO_2. Plasmid construction and cell transfection.

Human ITGA4 full-length cDNAs were amplified from human cDNA libraries and cloned into the pcDNA3.1–3xFlag-C (youbio). 1×10^5 cells/well were seeded on 6-well plates (Corning) one day before transfection and grown in supplemented RPMI-1640 at 37°C and 5% CO_2. When the cells grown to 70% confluence, plasmids were transfected with Lipofectamine LTX & Plus Reagent (Thermo Fisher Scientific). Transfection procedures were performed according to the manufacturer's standard protocol. The assays were performed at least five independent experiments, each performed in triplicate.

Cell Viability Assay

For cell viability, three GC cell lines, AGS, MKN45, and MGC803, with good growth status were digested with trypsin and resuspended by centrifugation. A total of 5000 cells/well were seeded into 96-well plates and 100 μL of the cell suspension was added to each well. The cells were cultured for 24 h and the culture medium was absorbed after the cells were completely adherent. Then, 100 μL of culture medium containing 5-FU at concentration gradients of 1.25, 2.5, 5, 10, 20, 40, 80, 160, 320, and 640 μg/mL was added. The control group (Con) was added to the culture medium without drugs. After 24 h, cell counting kit-8 (CCK-8) solution (Beyotime, C0038) was added, and the plates were incubated for 2–4 h. Then, Absorbance was measured at 450 nm using a Thermo Scientific Varioskan LUX multimode microplate reader. The data represented the mean of at least five independent experiments, with three replicates for each experiment. Cell survival rate (%) = [A (drug) − A (blank)] / [A (control) − A (blank)] × 100%.

Cell Proliferative Assay

500 cells/well were plated in 96-well plate, and cell viability was measured using the CCK-8 reagent at 0h, 24h, 48h, 72h, and 96h, with absorbance detection at 450nm. Data represent the average of at least five independent experiments, each performed in triplicate.

Colony Formation Experiments

The cells cultured during the logarithmic growth phase were suspended in complete medium containing 10% fetal bovine serum for later use. Each group of cells was seeded in a 6-well plate, with 300 cells evenly distributed in each well. Each group of cells was cultured at 37°C, 5% CO_2, and saturated humidity for 1 weeks. When visible colonies appear in the culture dish, terminate the culture, carefully aspirate the supernatant, wash twice with PBS, fix with 4% paraformaldehyde for 20 minutes, stain with crystal violet for 20 minutes, slowly wash off the staining solution with water, and then take photos. The cloning formation was calculated as the number of clones. Data represent the average of five independent assays, each performed in triplicate.

Apoptosis Assay

After cells were seeded at a density of 1.0×10^5 cells/well in a 6-well plate, each plate was treated with 5-FU (0, 10, 20 μg/mL) for 24 h. Then, the cells were washed twice with cold PBS and stained with Annexin V-FITC/PI kit (Beyotime, C1062S) according to the manufacturer's instructions. FACs was performed on a BD FACSCanto II cytometer (BD Biosciences) and the data were analyzed using Flow Jo 7.6.1 software (Tree Star, Inc., Ashland, OR). The data represent an average of six independent experiments, each performed in triplicate.

Wound Healing Assay

Cells were seeded at a density of 1.0×10^5 cells/well in a 6-well plate. At approximately 90% confluence, the cell layer was scratched using a 10μL sterile plastic pipette tip. The detached cells were rinsed twice with PBS, and RPMI-1640 medium containing 10% FBS was replaced with FBS-free RPMI-1640 medium. The cells were subsequently incubated for another 24 h with 2 mL/well of RPMI-1640 containing 5-FU. The control group consisted of wells that were not administered any drug (Con). At 0 h, 12 h and 24 h following treatment, scratches were photographed at 40× magnification and recorded using Image-Pro Plus 6.0. Finally, the migration rate (%) = [(Width 0 h – Width 12 h or 24 h)/Width 0 h] × 100% was used to calculate the migration rate. The data represented the mean of at least five independent experiments, with three replicates for each experiment.

Real-Time PCR

Total RNA was extracted from the cells using TRIzol Reagent (Invitrogen, 15596–026), and cDNA was synthesized using PrimeScript gDNA Eraser (Takara, RR047A). TB Green® Premix Ex Taq™ II (Tli RNaseH Plus) Kit (Takara, RR820L) was used for real-time PCR, which was performed the ABI7500 system under the following conditions: 95 °C for 5 s; 40 cycles of 95 °C for 5 s and 60 °C for 34s; and 95 °C for 15s, 60 °C for 60s, 95 °C for 30s, and 60 °C for 15s.

Each target gene and internal reference primers were designed using Primer Premier 5.0 (Table 1) and the relative expression level was calculated according to the formula of $2^{-\Delta\Delta ct}$. The data represent the average of at least five independent samples, each performed in triplicate.

Western Blotting

Proteins were extracted using RIPA lysis buffer (Beyotime, P0013C) containing a protease and phosphatase inhibitor cocktail (Beyotime, P1008). BCA assay kit (Beyotime, P0012) was used to determine the protein concentration of each sample. Total protein (20 μg) was separated using 10% SDS-PAGE and then transferred from the gel to a PVDF membrane. After blocking for 2h with skim milk (5%, w/v) in TBST, the primary antibodies against p-AKT-S473 (ABclonal, AP0637, 1:1000), AKT-1 (ABclonal, A17909, 1:2000), p-PI3K p85 (Tyr458) (Cell Signaling Technology, 4288T, 1:1000), PI3K (ABclonal, A4992, 1:2000), NR3C1 (Proteintech, 24050-1-AP, 1:3000) and GAPDH (ABclonal, A19056, 1:10000) were added to TBST with 5% skim milk and incubated with the membrane at 4 °C overnight. The membrane was washed and incubated with the corresponding secondary antibody HRP Goat anti-rabbit IgG (ABclonal, AS014, 1:5000) in TBST for 1h at room temperature. Finally, the protein blotting signals were detected using a super ECL plus agent (UElandy, S6009L), followed by imaging (Azure C600, Azure Biosystems) and analyses (Image-Pro Plus 6.0 software). Six independent cell experiments with technical triplicate.

Statistical Analysis

Statistical analysis was performed using GraphPad Prism 9.0 and IBM SPSS 26.0 (IBM, Armonk, NY, USA). The Shapiro–Wilk test and Q–Q chart was utilized to evaluate the data for normality. All the data were normally distributed, and the results are expressed as the means ± standard deviations (SDs). Then, we used Levene test to assess variance homogeneity. For data with homogeneity of variance, unpaired *t*-test was used for comparison between two groups, and one-way analysis of variance (ANOVA) and post-hoc Tukey ‘s test were used for comparison between multiple groups. For data with heteroscedasticity, the Welch ‘s *t*-test and Welch ‘s ANOVA was used to assess statistical significance. A P-value significance was set at $P < 0.05$.

Results

Potential GC-Related Therapeutic Mechanisms of 5-FU Through Network Pharmacological Analysis

Figure 1A shows the structural formula of 5-FU. A total of 36 5-FU targets were collected from ChEMBL and UniProt (Table S1). In total, 13,730 GC-related targets were obtained from the GeneCards database (20231107). By setting the

Table 1 Primer Sequences for Real-Time PCR

Gene symbols	Primer Sequences
NR3C1	Forward: 5’-AGTGGTTGAAAATCTCCTTAACTATTGCT-3’
	Reverse: 5’-GGTATCTGATTGGTGATGATTTCAGCTA-3’
DHFR	Forward: 5’-CTGTTTATAAGGAAGCCATGAATC-3’
	Reverse: 5’-ACACCTGGGTATTCTGGCAG-3’
CA2	Forward: 5’-TGGACTGGCCGTTCTAGGTATT-3’
	Reverse: 5’-CCAGCACATCAACAACTTTCTGA-3’
BCHE	Forward: 5’-ACAGGCCAGCTTGTGCTATT-3’
	Reverse: 5’-CAAAAGCCGAGGAAATTTTG-3’
ACHE	Forward: 5’-CTTGGTCAGGGGTGGTAGAC-3’
	Reverse: 5’-ATCTCGGTGCCCTCAAAACC-3’
ITGA4	Forward: 5’-TCGGAGCCAGCATACTACC-3’
	Reverse: 5’-CCACAGCACAGACAGAAGC-3’
GAPDH	Forward: 5’-GAAGGTGAAGGTCGGAGTC-3’
	Reverse: 5’-GAAGATGGTGATGGGATTTC-3’

https://doi.org/10.2147/DDDT.S474421

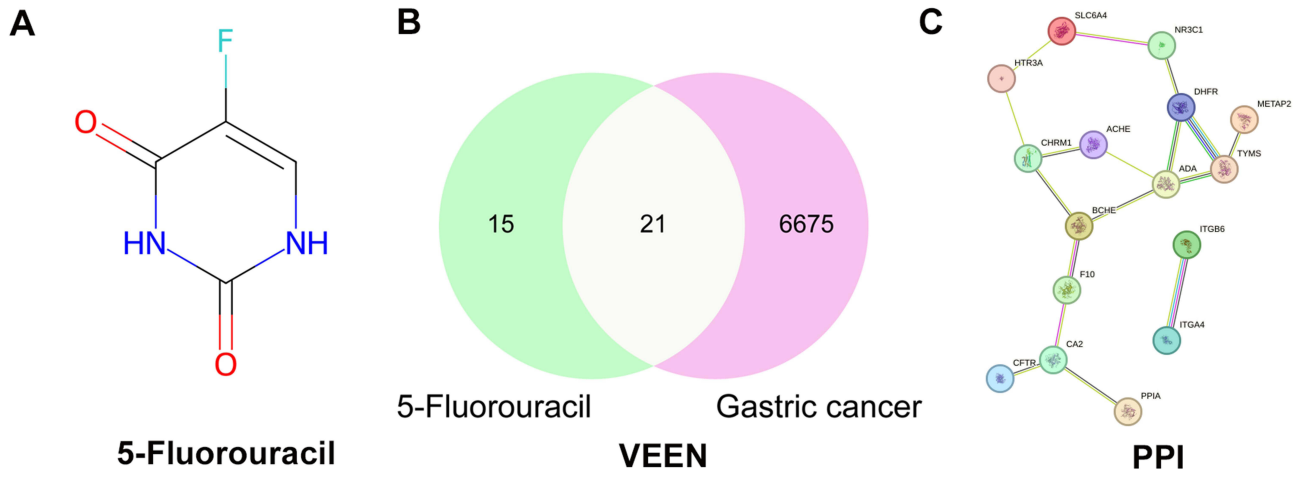

Figure 1 Target screening of 5-FU and GC. (**A**). Structural formula of 5-FU. (**B**) Venn diagram of 5-FU and GC. (**C**) PPI network of 5-FU and GC cross targets by the STRING database.

relevance score > median and deleting duplicate target genes, 6865 targets were obtained. Table S2 listed the top 200 GC-related targets obtained from the GeneCards database. Finally, 21 common targets of 5-FU and GC were obtained from Venny analysis (Figure 1B), as shown in Table 2.

The PPI network obtained using STRING is shown in Figure 1C. The PPI enrichment P value was less than 1.0e-16, where nodes represent proteins, each edge represents the interaction between proteins, and more lines represent a greater correlation. After removing the free points, 16 targets and 17 edges were identified, and the average node degree was 2.13. The.tsv file downloaded from STRING was processed in Cytoscape and assessed by "cytohubba" According to the ascending order of the values of degree, betweenness, and closeness, three common genes with the top five minimum values were eliminated, and 13 candidate target genes were identified (Table 3).

Table 2 Details of Shared 5-FU and GC Targets

NO.	Target	Symbol	UniProt ID
1	Butyrylcholinesterase	BCHE	P06276
2	Coagulation Factor X	F10	P00742
3	Nuclear Receptor Subfamily 3 Group C Member 1	NR3C1	P04150
4	5-Hydroxytryptamine Receptor 3A	HTR3A	P46098
5	Cholinergic Receptor Muscarinic 1	CHRM1	P11229
6	Protein Tyrosine Phosphatase Non-Receptor Type 2	PTPN2	P17706
7	Thymidylate Synthetase	TYMS	P04818
8	Phosphodiesterase 5A	PDE5A	O76074
9	Methionyl Aminopeptidase 2	METAP2	P50579
10	Integrin Subunit Beta 6	ITGB6	P18564
11	Acetylcholinesterase (Cartwright Blood Group)	ACHE	P22303
12	CF Transmembrane Conductance Regulator	CFTR	P13569
13	Dihydrofolate Reductase	DHFR	P00374
14	Prostaglandin E Receptor 4	PTGER4	P35408
15	ROS Proto-Oncogene 1, Receptor Tyrosine Kinase	ROS1	P08922
16	Solute Carrier Family 6 Member 4	SLC6A4	P31645
17	Peptidylprolyl Isomerase A	PPIA	P62937
18	Adenosine Deaminase	ADA	P00813
19	Integrin Subunit Alpha 4	ITGA4	P13612
20	Coactivator Associated Arginine Methyltransferase 1	CARM1	Q86X55
21	Carbonic Anhydrase 2	CA2	P00918

Table 3 List of Targets of 5-FU Therapy for GC From PPI Network

NO.	Target	Degree	Closeness	Betweenness
1	ADA	4	0.034483	61.66666667
2	BCHE	3	0.035714	78.33333333
3	CHRM1	3	0.030303	33.66666667
4	DHFR	3	0.029412	25.33333333
5	TYMS	3	0.027778	24
6	CA2	3	0.02381	46
7	F10	2	0.029412	60
8	ACHE	2	0.027778	6.333333333
9	HTR3A	2	0.025	16
10	NR3C1	2	0.02439	11.33333333
11	SLC6A4	2	0.023256	7.333333333
12	ITGA4	1	1	0
13	ITGB6	1	1	0

GO enrichment and KEGG enrichment analysis were performed on 13 candidate targets by Sangerbox (http://vip.sangerbox.com/login.html). GO enrichment analysis identified 642 significant items, including 499 BP, 52 CC, and 91 MF, mainly including response to drug, trans-synaptic signaling, integral component of presynaptic membrane, and ammonium ion binding (Figure 2A–C). The top 15 BP, CC, and MF in GO enrichment were plotted in Table S3–5 ($P < 0.05$).

KEGG pathway enrichment analysis revealed 15 important pathways, including one carbon pool by folate, regulation of actin cytoskeleton, and the PI3K/AKT signaling pathway (Figure 2D and Table S6).

Molecular Docking Analysis

The results of molecular docking further verified the role of 5-FU in GC and network pharmacology. Molecular docking of 13 targets with 5-FU was performed. When the binding energy of the molecules and proteins was less than 0, it indicated that it could be carried out spontaneously, and the inhibition constant (Ki) was used as a reference. Table 4 lists the binding energies and inhibition constants of each target molecule. It can be seen that the docking result of F10 is the best, which is −4.50 kcal/mol, NR3C1 is −4.44 kcal/mol, DHFR is −4.24 kcal/mol, CA2 is −4.20 kcal/mol, BCHE is −3.93 kcal/mol, ACHE is −3.68 kcal/mol, ITGA4 is −3.64 kcal/mol, and the results are imported into PyMOL for visualization (Figure 3). Targets with binding energies beyond the median value were considered the core targets of 5-FU in GC treatment in this study. Therefore, F10, NR3C1, DHFR, CA2, BCHE, ACHE, and ITGA4 were selected as the core genes for further investigation.

Bioinformatics Analysis

The boxplot reveals the expression of seven core targets in GC compared to normal cells. The mRNA expression of CA2 was lower in GC tissues versus normal tissues; in contrast, the mRNA levels of DHFR, ACHE, and IGTA4 were higher in GC tissues ($p< 0.05$, Figure 4A). In addition, a correlation analysis of the mRNA expression of core targets with the progression of GC revealed that NR3C1 and IGTA4 were markedly altered with the development of GC (Figure 4B). Furthermore, the survival curve obtained from the Kaplan-Meier plotter indicated that patients with high expression of DHFR and CA2 had a better prognosis versus those with low expression. In contrast, patients with high F10, NR3C1, BCHE, and ACHE expression had poorer prognosis than those with low expression (Figure 4C).

Molecular Dynamics Simulations

The root mean square distance/deviation (RMSD) was used to measure the difference between different conformations of the same molecular structure. It is the root mean square of the distance between all the corresponding atoms after the position overlap of the two conformations. The specific formula is as follows:

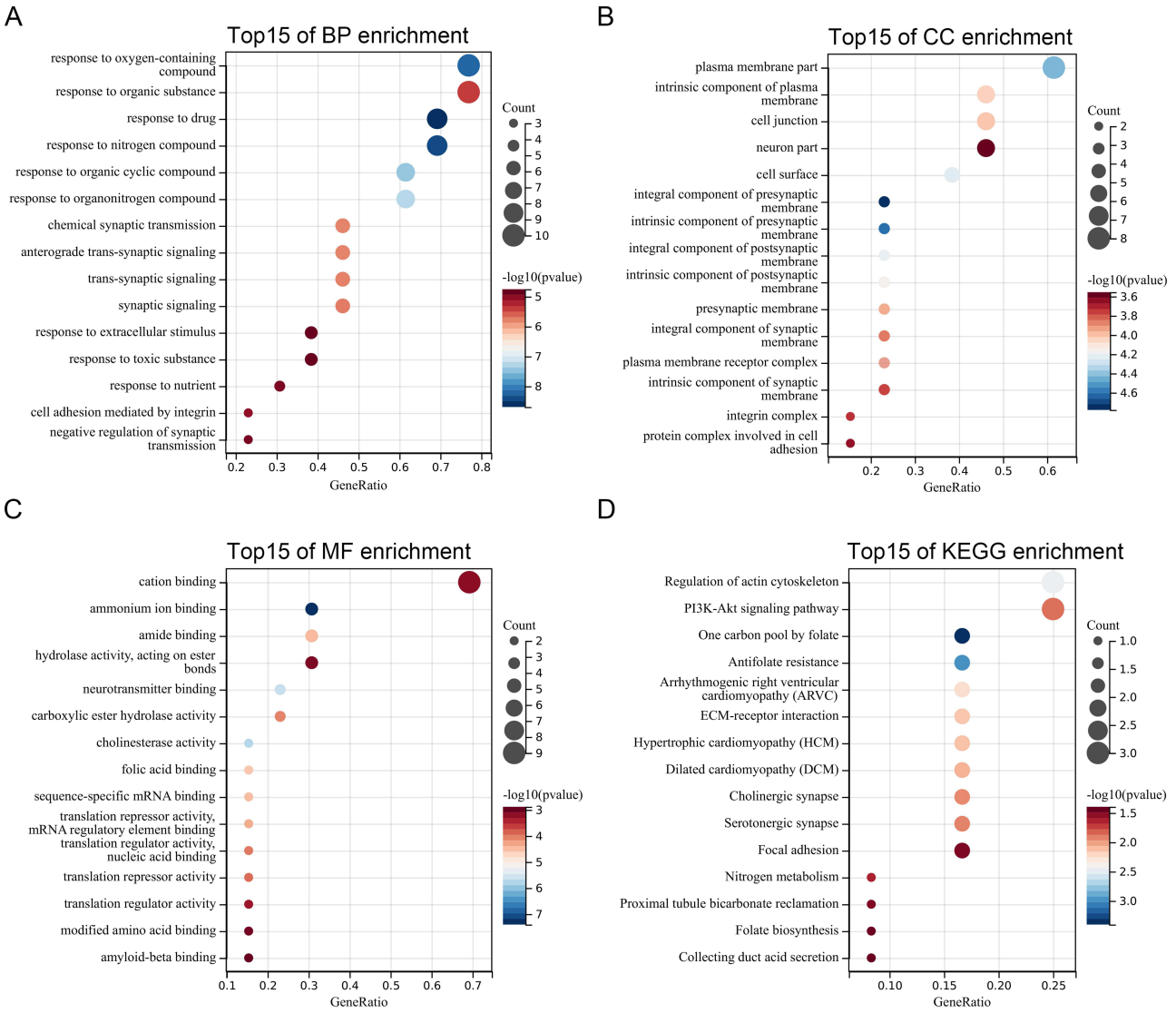

Figure 2 GO and KEGG enrichment analysis for 5-FU and GC cross targets performed via Sangerbox. (**A**)The top 15 significant biological process (BP), (**B**) The top 15 significant cellular component (CC), and (**C**) the top 15 significant molecular function (MF) of GO enrichment; (**D**) KEGG pathway enrichment analysis of the cross targets.

$$RMSD(t) = \sqrt{\frac{1}{n}\sum_{t=1}^{N}\left(r_i(t) - r_i^{ref}\right)^2}$$

RMSD is often used to analyze the stability of the overall molecular structure of a system. A decrease in RMSD indicates that the structure tends to be stable and vice versa. Figure 5A and E, from top to bottom show the NR3C1–5-FU complex

Table 4 Binding Affinities of Active Ingredients and Core Targets

Target	PDB ID	Binding Energy (kcal/mol)	Inhibition Constant
F10	3KL6	−4.50	506.24
NR3C1	4UDD	−4.44	557.15
DHFR	4G95	−4.24	778.38

(*Continued*)

Table 4 (Continued).

Target	PDB ID	Binding Energy (kcal/mol)	Inhibition Constant
CA2	6VJ3	−4.20	835.7
BCHE	6QAA	−3.93	1.31
ACHE	4EY8	−3.68	2.00
ITGA4	3V4V	−3.64	2.13
ITGB6	5FFG	−3.54	2.56
SLC6A4	5I71	−3.48	2.19
ADA	3IAR	−3.34	3.58
CHRM1	5CXV	−3.20	4.49
TYMS	5HS3	−3.17	4.78
HTR3A	–	–	–

Note: No corresponding structure found in the RCSB Protein Data Bank (PDB).

and ITGA4–5-FU complex. The RMSD of the two proteins fluctuated greatly from the beginning of the simulation to 20 ns, and then, with gradual stabilization, the simulation reached the equilibrium state. The observation trajectory revealed that this was because the small molecule separated from the original pocket and then entered the new pocket.

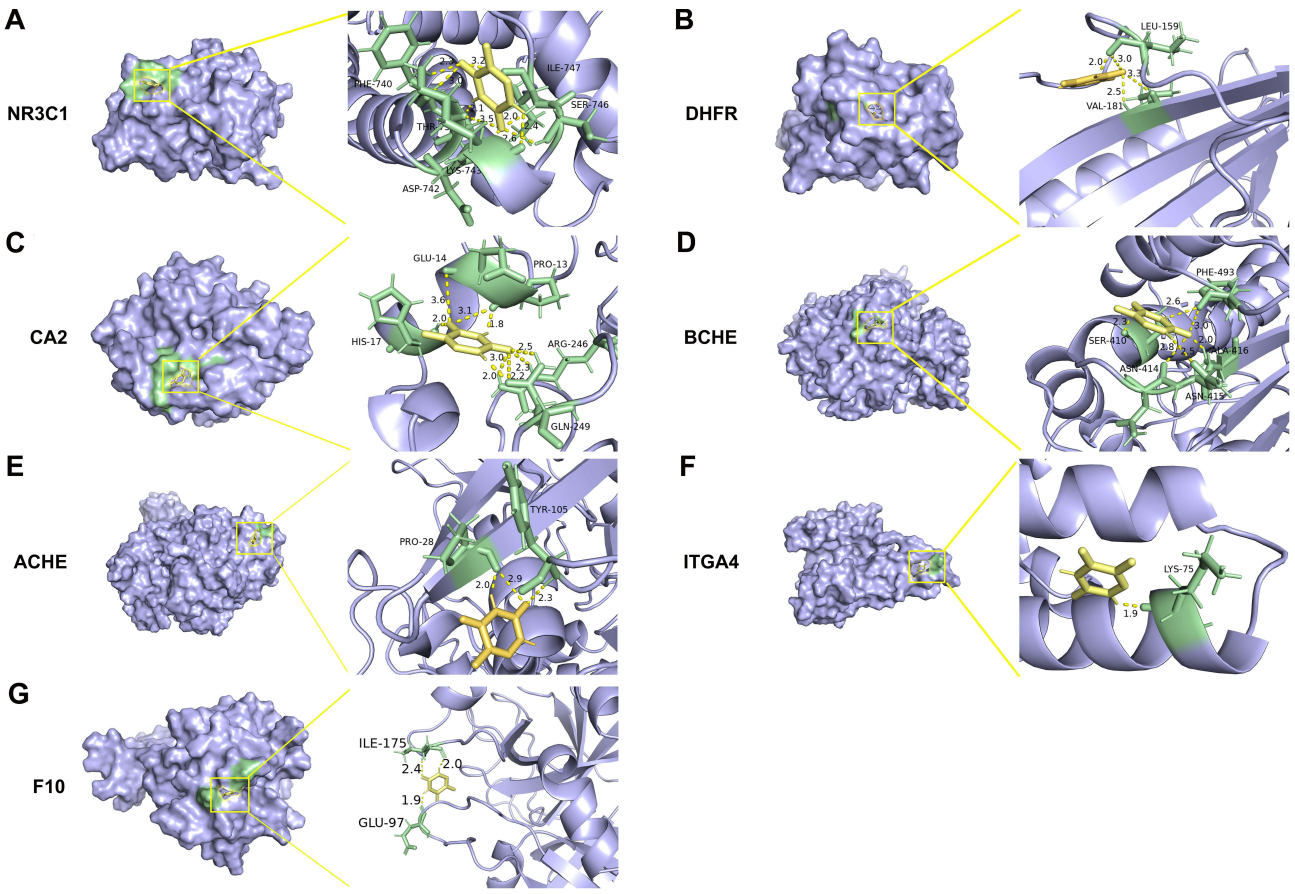

Figure 3 Pattern diagram of molecular docking. (**A**) Molecular docking of 5-FU and NR3C1, (**B**) Molecular docking of 5-FU and DHFR, (**C**) Molecular docking of 5-FU and CA2, (**D**) Molecular docking of 5-FU and BCHE, (**E**) Molecular docking of 5-FU and ACHE, (**F**) Molecular docking of 5-FU and ITGA4, (**G**) Molecular docking of 5-FU and F10. The left side shows the 3D structure of the target protein, the yellow box represents the binding pocket structure, and the right side shows the enlarged display of the binding pocket. The yellow part represents 5-FU, the green part represents the binding residue, the dashed line represents the hydrogen bond, and the text part represents the residue name.

https://doi.org/10.2147/DDDT.S474421

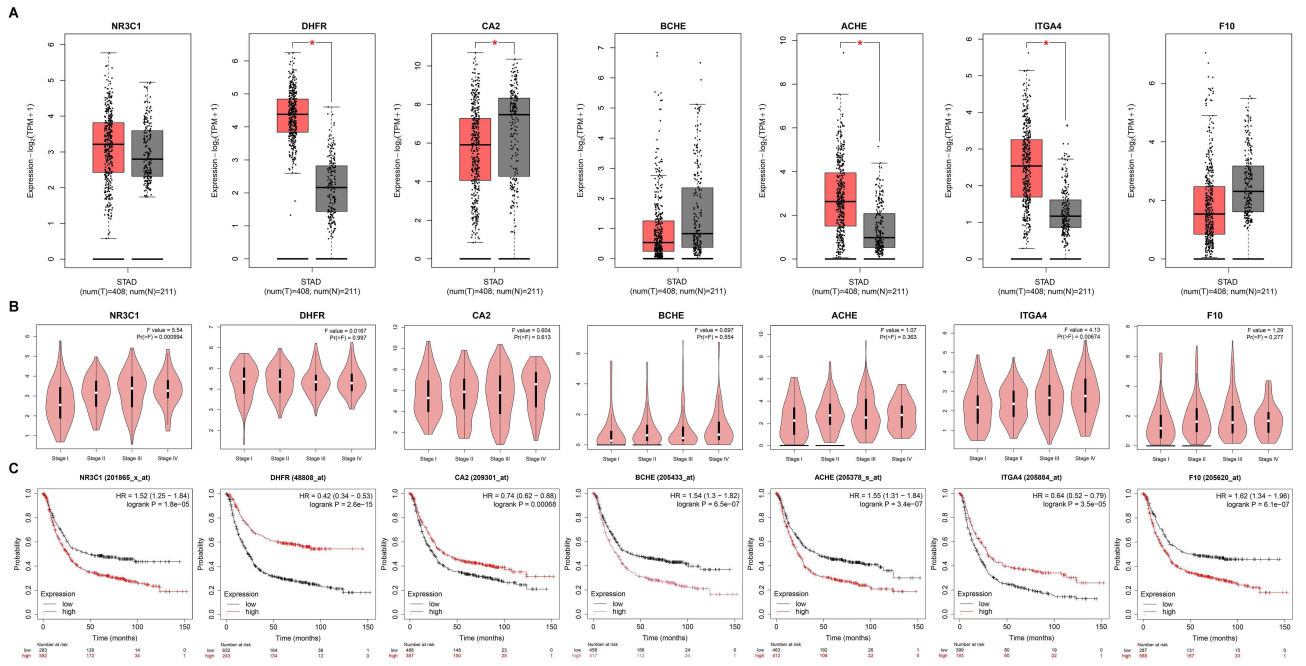

Figure 4 mRNA expression level, pathological stage of Hub targets in the GEPIA database and OS in the Kaplan–Meier Plotter. (**A**) Box plots showing the mRNA expression levels of NR3C1, DHFR, CA2, BCHE, ACHE, ITGA4 and F10. Red represents Tumor, Gray represents normal. * P <0.05. (**B**) The violin diagram shows the stage plot of NR3C1, DHFR, CA2, BCHE, ACHE, ITGA4 and F10 mRNA expression level and pathological stage in the GEPIA database. (**C**) The line charts show the OS of hub genes NR3C1, DHFR, CA2, BCHE, ACHE, ITGA4 and F10 in the Kaplan–Meier Plotter. The survival curve comparing the patients with high (red) and low (black) expression in GC.

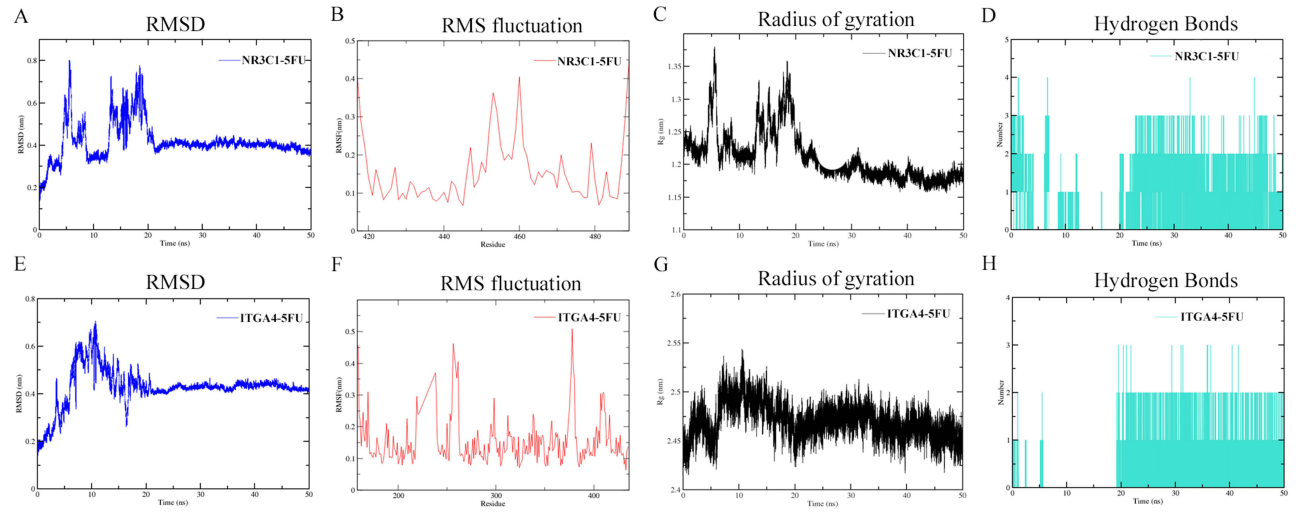

Figure 5 Molecular dynamics simulation (**A**–**D**) RMSD, RMS fluctuation, Radius of gyration, Hydrogen bonds of NR3C1 and 5-FU; (**E**–**H**) RMSD, RMS fluctuation, Radius of gyration, Hydrogen bonds of ITGA4 and 5-FU.
Abbreviations: RMSD, root mean squared error; RMS fluctuation, root mean square fluctuations.

Root mean square fluctuation (RMSF) was used to measure the average movement of the atomic position in the molecular structure over a period. It is the root mean square of the distance between a specific atom of the target structure and the reference structure over the entire time range. The specific formula is as follows:

$$RMSF_I = \sqrt{\frac{1}{T}\sum_{t=1}^{N}\left(r_i(t) - r_i^{ref}\right)^2}$$

As shown in Figure 5B and F, the RMS values of the NR3C1–5-FU complex and ITGA4–5-FU complex are displayed from top to bottom. The amino acids near 417–419,452-461,479 and 488–489 in NR3C1–5-FU had higher flexibility, and the amino acids near 159,169,219,238–239,255-261,375–380 and 407–410 in ITGA4–5-FU had higher flexibility.

Radius of gyration (Rg) was used to measure the tightness or folding degree of the molecular structure. It is the average distance of all atoms of the molecule relative to the centre of mass. The specific formula is as follows:

$$Rg = \sqrt{\frac{1}{N}\sum_{i=1}^{N}(r_i - r_{com})^2}$$

Figure 5C shows that the Rg of NR3C1–5-FU cells changed significantly in the 0–20 ns stage. Combined with RMSD, it can be seen that the change was concentrated in the stage of 5-FU breaking away from the original pocket and rebinding to the protein, and gradually decreased after binding to the new site, and the system tended to be dense. This was also the case for the ITGA4–5-FU interaction (Figure 5G). After 20 ns, the system tended to become dense. At this time, the structure could be observed because 5-FU tended to be stable at the new binding site.

In the simulation process, small molecules formed a certain number of hydrogen bonds with proteins. GROMACS uses geometric criteria to determine the hydrogen bonds. When the hydrogen bond donor was less than 3.5 Å and the angle of the hydrogen donor receptor was less than 30°, it was determined to be a hydrogen bond. As shown in Figure 5D and H, from top to bottom are the NR3C1–5-FU complex and ITGA4–5-FU complex. It can be seen from the diagram that during the simulation process, in ITGA4–5-FU, hydrogen bonds were not observed most of the time before 20 ns, which was due to the detachment of small molecules from the protein. At least two hydrogen bonds were maintained most of the time at approximately 20–50 ns. Hydrogen bonds between proteins and small molecules are also an important factor in their stable binding, indicating that the binding of proteins and small molecules is stable There were at least two hydrogen bonds between the small molecules and proteins in NR3C1–5-FU most of the time when the simulation was carried out for 20–50 ns. At this time, 5-FU was located in the new pocket, and the binding of 5-FU to the protein was relatively stable.

5-FU Promoted Apoptosis and Inhibits Cell Migration in AGS via the PI3K/AKT Pathway

To comprehend the mechanism underlying the impact of 5-FU, in vitro experiments were conducted to assess the influence of 5-FU on a pivotal cell survival, cell growth pathway, namely the PI3K/AKT pathway, which serves as a central mediator of oncogenesis. Firstly, the CCK-8 assay was utilized to assess cell viability with 5-FU treatment with 24h. Compared with the untreated group (Con), 5-FU treatment inhibited cell proliferation in a dose-dependent manner (Figure 6A). Compared with MKN-45 and MGC-803 cells, 5-FU had the most obvious inhibition effect on AGS cells, with an IC_{50} value of 14.60 μg/mL (Figure 6B). As a result, 5-FU concentrations of 10 and 20 μg/mL were selected for future investigations.

Real-time PCR assay was used to observe the expression of target genes predicted by network pharmacology. Among all targets, BCHE was excluded because of its undetectable expression levels. As shown in Figure 6C, ACHE, ITGA4, NR3C1, and CA2 exhibited significant changes following 5-FU treatment, whereas DHFR and F10 did not. Further Western blot tests demonstrated that the protein levels of ITGA4 and NR3C1 also upregulated following the 5-FU treatment (Figure 6D).

Furthermore, the apoptosis analysis and wound healing experiments demonstrated that 5-FU significantly enhances the cell apoptosis (Figure 6E) and inhibited cell migration in AGS cells (Figure 6F). Western blot analysis showed that 5-FU inhibited the expression of p-PI3K and p-AKT in AGS cells in a dose-dependent manner (Figure 6G). Combined with the network pharmacology results, all these results suggested that 5-FU treatment inhibits the malignant behaviour of GC cells, partially due to the regulation of the PI3K/AKT pathway.

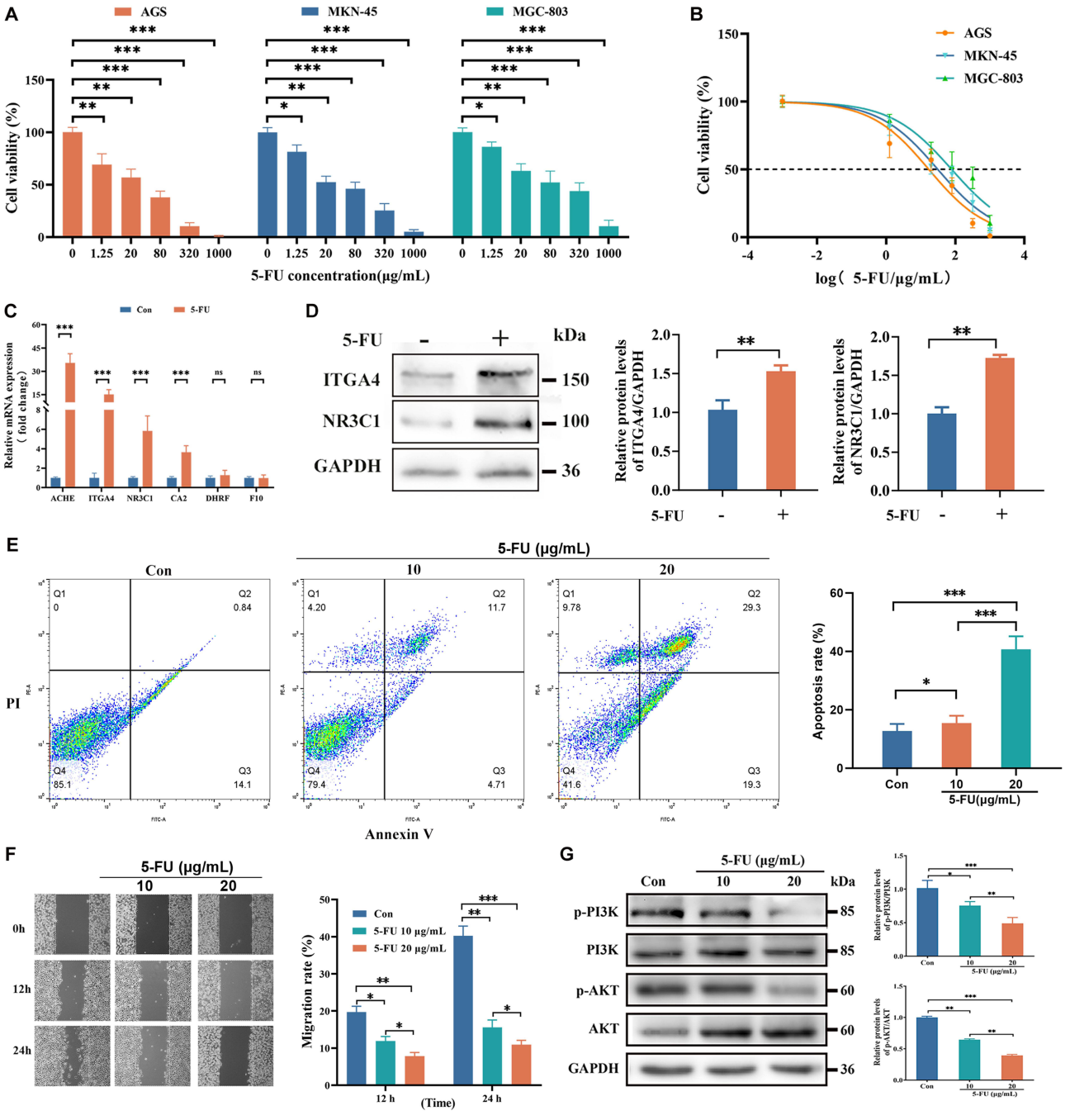

Figure 6 The effect of 5-FU on GC was verified by experiment. (**A** and **B**) The effects of 5-FU treatment for 24 hours were detected by CCK-8 assay (N=6). *P < 0.05, **P < 0.01, ***P < 0.001 by One-way ANOVA. (**C**) Changes in the mRNA expression levels of Hub genes in AGS cell lines. Gene expression was evaluated by real-time PCR, using the $2^{-\Delta\Delta CT}$ method (N=6). ***P < 0.001, ns, no significance P > 0.05 by t-test. (**D**) ITGA4, NR3C1 were detected by Western blot (N=6). **P < 0.01 by t-test. (**E**) Effects of 5-FU (10, 20 μg/mL, 24 h) on the apoptosis of AGS was assessed using an Annexin V-FITC/PI dual staining detection kit (N=6). *P < 0.05, ***P < 0.001 by One-way ANOVA. (**F**) Cell migration assessed through wound healing assay (N=6). *P < 0.05, **P < 0.01, ***P < 0.001 by One-way ANOVA. (**G**) p-PI3K, PI3K, p-AKT, and AKT protein levels were detected by Western blot (N=6). *P < 0.05, **P < 0.01, ***P < 0.001 by One-way ANOVA. Data are expressed as mean ± SD. CCK-8, cell count kit 8; 5-FU, 5-fluorouracil; SD, standard deviation; Con, Negative control group; -, without 5-FU treated; +, with 20 μg/mL 5-FU treated.

ITGA4 Overexpression Promotes Proliferation, Migration in AGS Cell

To further verify the ITGA4 function in vitro, AGS cells were transfected with ITGA4-pcDNA3.1–3xFlag-C plasmid (OE-ITGA4) and pcDNA3.1–3xFlag-C plasmid (OE-NC), respectively. The results of real-time PCR (data not shown) and Western blot indicated that ITGA4 was successfully upregulated (Figure 7A). The CCK-8 assay showed that the ability of cell proliferation increased significantly in OE-ITGA4 cells (Figure 7B). Similar results were obtained in cell

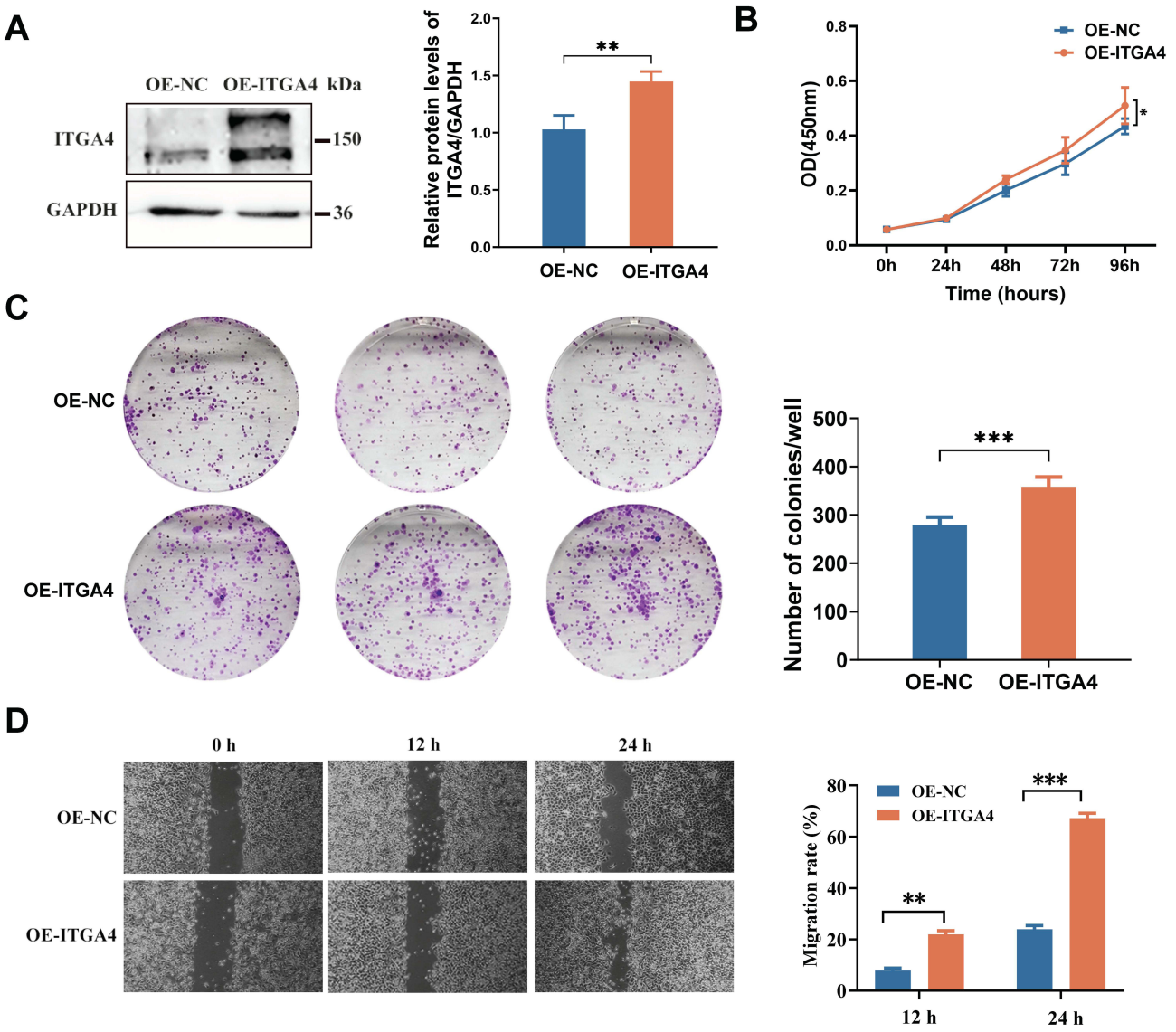

Figure 7 ITGA4 overexpression promotes proliferation and migration. (**A**) ITGA4 overexpression identified by Western blot (N=6). $^{**}P < 0.01$ by *t*-test. (**B**) Cell viability detected by cell proliferation assay (N=5). $^{*}P < 0.05$ by *t*-test. (**C**) Cell proliferation performed by colonies formation (N=5). $^{***}P < 0.001$ by *t*-test. (**D**) Cell migration assessed through wound healing assay (N=6). $^{**}P < 0.01$, $^{***}P < 0.001$ by *t*-test. Data are expressed as mean ± SD. OE-NC, AGS cells were transfected with pcDNA3.1–3xFlag-C plasmid; OE-ITGA4, AGS cells were transfected with ITGA4-pcDNA3.1–3xFlag-C plasmid.

cloning experiments using 300 cells / well in 6-well plates (Figure 7C). Besides, wound healing assay showed that the migration ability of OE-ITGA4 cells were also significantly enhanced (Figure 7D). All these data showed that ITGA4 overexpression in AGS cells may play an antagonistic role in the drug response to 5-FU.

ITGA4 Overexpression Upregulates the Anti-Apoptotic Capacity and Resistance of 5-FU

In the present study, we are concentrating on the changes caused by the rise in ITGA4 in GC cells following 5-FU therapy. The apoptosis assays and the cytotoxicity tests were conducted. As shown in Figure 8A and B, compared with OE-NC cells, the anti-apoptotic ability of OE-ITGA4 cells was significantly enhanced after induction with 10 μg/mL or 20 μg/mL 5-FU. Besides, the IC_{50} value of the OE-ITGA4 AGS cells was 19.79 μg/mL (Figure 8C), which was significantly higher than that in OE-NC AGS cells (12.86 μg/mL). All these findings suggested that the increased ITGA4 may contribute to cell survival and 5-FU resistance.

https://doi.org/10.2147/DDDT.S474421

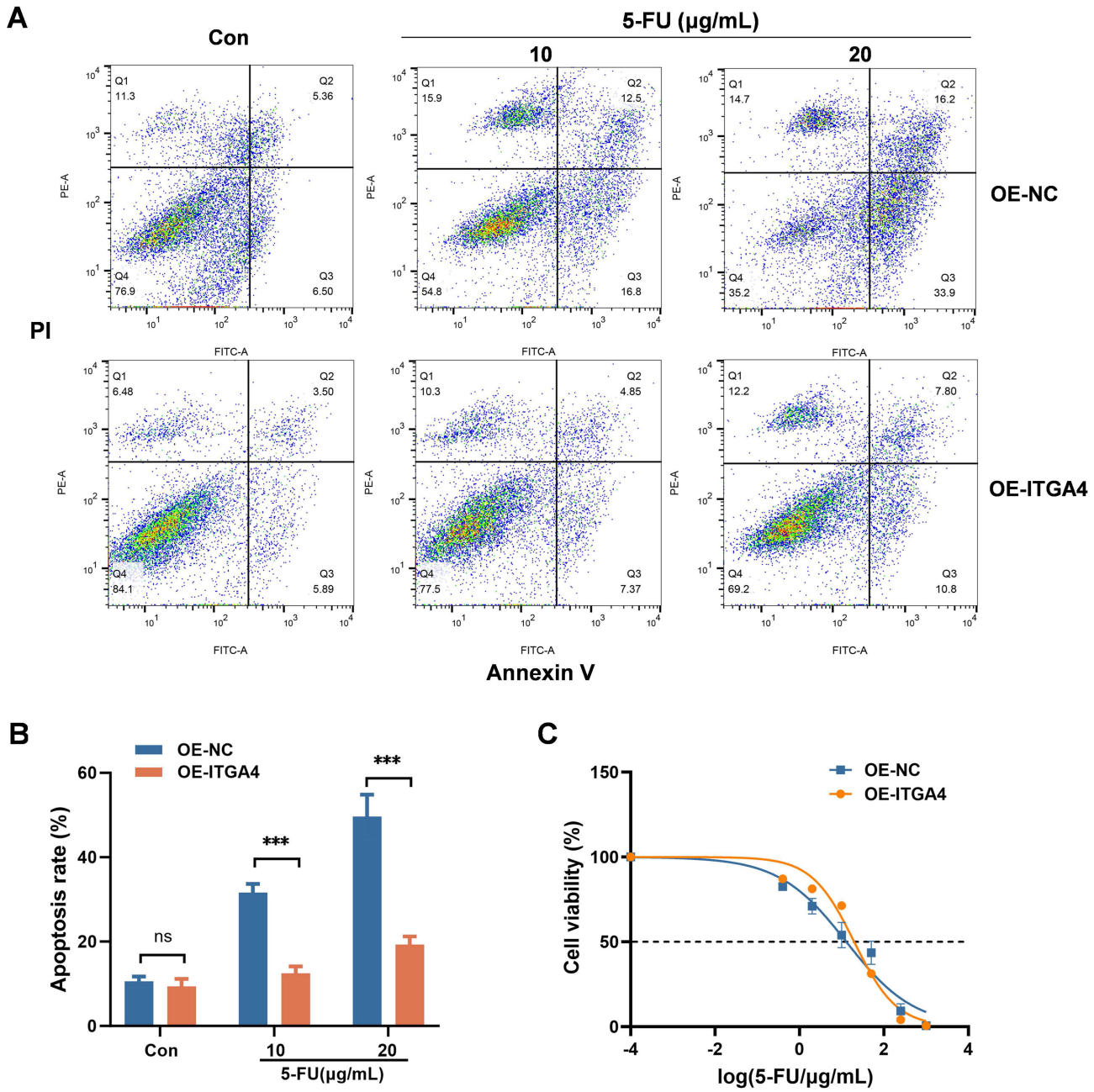

Figure 8 ITGA4 overexpression promotes anti-apoptotic capacity and 5-FU resistance. (**A** and **B**) Cell apoptosis assessed using an Annexin V-FITC/PI dual staining detection (N=6). ***$P < 0.001$, ns, no significance $P > 0.05$ by *t*-test. (**C**) IC_{50} detected in OE-NC and OE-ITGA4 AGS cells (N=6). Data are expressed as mean ± SD. OE-NC, AGS cells were transfected with pcDNA3.1–3xFlag-C plasmid; OE-ITGA4, AGS cells were transfected with ITGA4-pcDNA3.1–3xFlag-C plasmid.

PI3K/AKT Signaling is Required for the Function of ITGA4 in AGS Cell

To further test whether ITGA4 overexpression counteracts the drug response to 5-FU through the PI3K/AKT pathway, the cells were divided into four groups: OE-ITGA4, OE-NC, OE-ITGA4 cells under the exposure of 0.25 nM CAP (OE-ITGA4+CAP), and OE-NC cells under the exposure of 0.25 nM CAP (OE-NC+CAP). Consequently, the expression of p-AKT/AKT significantly increased in OE-ITGA4 cells, and after adding CAP, the expression of p-AKT/AKT correspondingly decreased (Figure 9). Meanwhile, after adding CAP, the IC_{50} levels of OE-NC+CAP and OE-ITGA4+CAP AGS cells dramatically decreased compared with OE-NC AGS cells, showing higher sensitivity to 5-FU. The above results suggested that ITGA4 overexpression mediates the PI3K/AKT pathway to enhance protective activity and partially promote resistance to 5-FU.

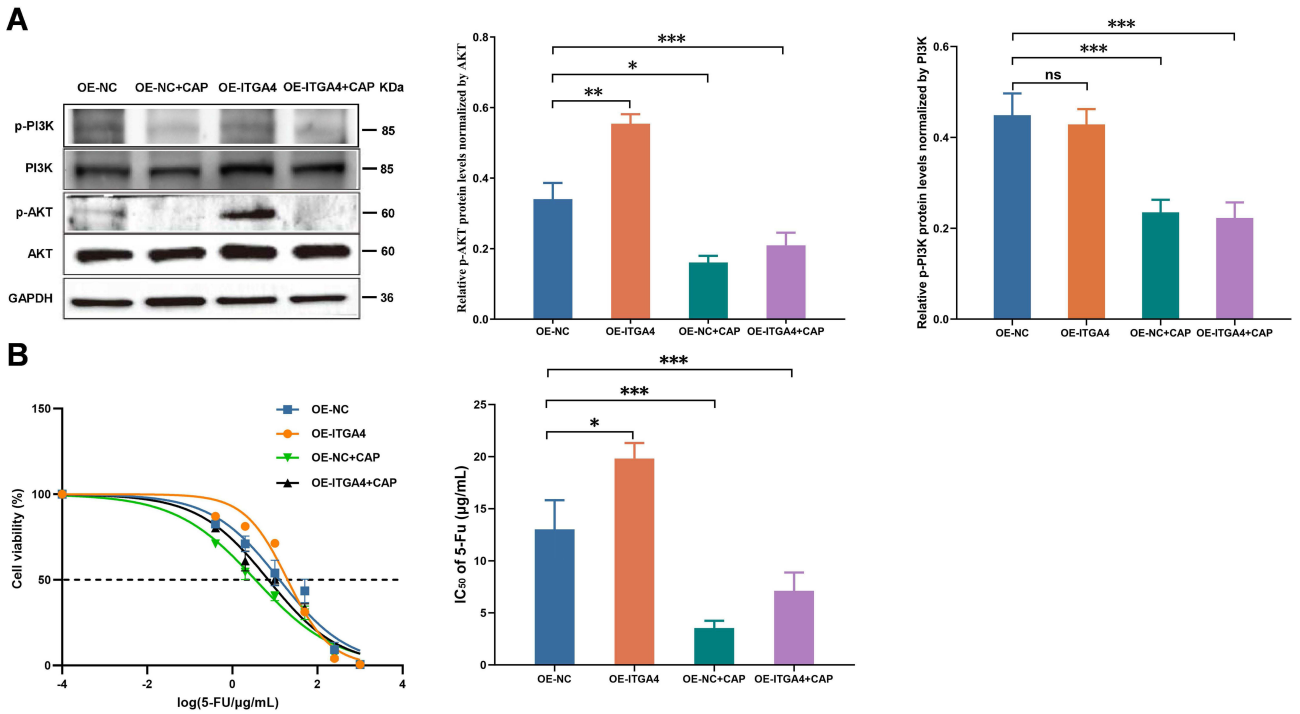

Figure 9 PI3K/AKT signaling is required for the function of ITGA4. (**A**) Western blot for p-PI3K, PI3K, p-AKT, AKT (N=6). *P < 0.05, **P < 0.01, ***P < 0.001, ns, no significance P > 0.05 by One-way ANOVA. (**B**) IC_{50} detected in OE-NC+CAP and OE-ITGA4+CAP AGS cells (N=6). *P < 0.05, ***P < 0.001 by One-way ANOVA. Data are expressed as mean ± SD. CAP, capivasertib; OE-NC+CAP, AGS cells were transfected with pcDNA3.1–3xFlag-C plasmid cultured with 0.25 nM CAP; OE-ITGA4+CAP, AGS cells were transfected with ITGA4-pcDNA3.1–3xFlag-C plasmid cultured with 0.25 nM CAP.

Discussion

Network pharmacology is a new research field that integrates multiple platforms and technologies. By constructing a variety of network models, the correlation between the targets of the components and the disease can be effectively and systematically explored, and the mechanism of action can be explained. In this study, we utilized network pharmacology to identify potential drug targets and pathways for 5-FU in treating GC, subsequently conducting in vitro validation. To our knowledge, network pharmacology is primarily used to investigate the mechanisms of traditional Chinese medicine and natural compounds in diseases. Our study is the first to use a network pharmacology system to elucidate the mechanism of 5-FU action on GC. Our research has also identified several novel potential drug targets, such as ACHE, ITGA4, NR3C1, etc. It is particularly noteworthy that ITGA4 expression increased in GC AGS cells after 5-FU treatment. The elevated ITGA4 activated the PI3K/AKT pathway, demonstrating stronger cell viability and higher 5-FU resistance.

Thirty-six targets of 5-FU were collected from multiple databases, and 21 targets related to GC were obtained using a Venn diagram. According to the STRING database protein interaction network and Cytoscape analysis, the targets were ranked as ADA, BCHE, and CHRM1, indicating the possible molecular mechanism of 5-FU against GC. To elucidate the mechanism of action of 5-FU in the treatment of GC, GO functional enrichment and KEGG pathway analyses were performed on the targets using the Sangerbox tool (Figure 2). It was found that the GO enrichment analysis of 5-FU in the treatment of GC involved response to drug, trans-synaptic signaling, integral components of the presynaptic membrane, and ammonium ion binding. In addition, KEGG analysis revealed that GC-related genes were related to the regulation of one carbon pool by folate, regulation of the actin cytoskeleton, and the PI3K/AKT signaling pathway. Most of the results obtained by the GO and KEGG pathway enrichment analyses were related to cancer.

Subsequently, molecular docking was conducted to assess the potential binding affinity of 5-FU for shared targets. Targets NR3C1, DHFR, CA2, BCHE, ACHE, and ITGA4, which exhibited binding energies below the median value, were identified as core genes for subsequent analysis. Bioinformatics analysis data showed that the mRNA levels of NR3C1, DHFR, ACHE, and IGTA4 were significantly expressed in GC tissues, and the levels of NR3C1 and IGTA4

https://doi.org/10.2147/DDDT.S474421

changed significantly with pathological stage. Therefore, NR3C1 and ITGA4 were selected for validation in subsequent Molecular simulation assays. In addition, higher expression levels of NR3C1 were linked to a poor prognosis versus those with low expression ($P < 0.05$), in agreement with findings from previous reports.[16,17]

In addition, in vitro experiments were conducted to assess the effects of 5-FU on GC. Using the CCK8 assay, we observed that cell proliferation was dose-dependently inhibited, with the AGS cell line exhibiting the most pronounced inhibitory effect among the three cell lines tested.[18] Consequently, the AGS cell line was used for further analysis. To observe the expression of target gene predicted by network pharmacology, real-time PCR and Western blot analysis were tested. The results showed that a significant increase in mRNA and protein levels of ITGA4 and NR3C1 occurred after 5-FU treatment (Figure 6C and D). The mechanism of 5-FU action through the PI3K/AKT pathway was also explored because of the altered levels of ITGA4 and NR3C1 and their involvement in the PI3K/AKT pathway. 5-FU significantly inhibited the expression of p-PI3K and p-AKT without significant changes in PI3K and AKT protein levels, respectively.[19] Inhibition of the PI3K/AKT signaling pathway by 5-FU effectively attenuated proliferation and migration and enhanced apoptosis in AGS cells (Figure 6).[20]

Integrin α4 (ITGA4) is a member of the integrin protein family. Previous studies have demonstrated that ITGA4 is overexpressed in certain immune disorders and nervous system malignancies[21,22] and plays a role in cellular processes, such as motility, adhesion, and migration.[23] Darzi et al discovered that downregulation of ITGA4 may be a potential therapeutic application in cancer.[24] De Lange et al found that ITGA4 is involved in cell surface adhesion and signal transduction, making it a common therapeutic target for Crohn's disease and inflammatory bowel disease (IBD).[25] Furthermore, Xie et al illustrated that the downregulation of ITGA4 results in the suppression of Hh pathway activation, thereby diminishing PI3K/AKT signaling, suggesting a critical involvement of ITGA4 in the PI3K/AKT pathway.[26] To further verify the function of the core target gene ITGA4 in GC treatment, ITGA4 was overexpressed in vitro. The results showed that the ITGA4 mRNA and protein levels were successfully overexpressed in AGS cells and were involved in cell proliferation and invasion, which was consistent with previous studies.[27] However, in the present study, we are concentrating on the changes caused by the rise in ITGA4 in GC cells following 5-FU therapy. Subsequently, apoptosis assays and the cytotoxicity tests were performed to observe the alterations caused by the rise in ITGA4 in GC cells following 5-FU therapy. Interestingly, cells overexpressing ITGA4 exhibited increased anti-apoptosis ability and enhanced 5-FU resistance. Moreover, the expression of p-AKT/AKT in ITGA4 upregulated cells significantly increased, while it correspondingly decreased after the addition of CAP. At the same time, a decrease in IC_{50} was observed in the cells treated with CAP. All these data indicated that upregulated ITGA4 expression in AGS cells improved cell survival and showed resistance to 5-FU via PI3K/AKT pathway. These findings provide new insights into whether ITGA4 inhibitors can be served as a synergistic treatment in combination with 5-FU for GC.

Typically, 5-FU inhibits tumor growth by disrupting DNA and RNA synthesis.[28] However, our study used network pharmacology to find that 5-FU treatment increases ITGA4 expression, partially offsetting the therapeutic effect. In clinical practice, GC diseases are mostly treated with 5-FU-based regimens like S-1 plus oxaliplatin (SOX) and capecitabine plus oxaliplatin (XELOX), which greatly enhanced the effectiveness of treatment.[29,30] Thus, ITGA4 inhibitors or ITGA4-based treatment strategies may provide opportunities for drug research and discovery to improve the efficacy of patients with GC.

Nevertheless, it is important to acknowledge the limitations associated with predicting the effective components and targets of 5-FU using network pharmacology because reliance solely on existing databases may yield varying results. It is advisable to use multiple databases to enhance the comprehensiveness of network predictions. Furthermore, given the diverse range of GC cell lines, conducting experiments using multiple cell lines concurrently may provide valuable insights for future research. Besides, this study did not validate the function and mechanism of the target gene ITAG4 of 5-FU in vivo. Therefore, further research should be conducted in various cell lines and in vivo to explore and develop the feasibility of ITGA4 inhibitors as a synergistic treatment of 5-FU for GC clinical application.

Conclusion

In conclusion, the present study showcased a viable network pharmacology approach to uncover the multi-target and multi-pathway effects of 5-FU in treating GC, emphasizing the key role of core targets ITGA4 and the classical pathway

PI3K/AKT under 5-FU exposure. First, ITGA4 expression at both mRNA and protein levels was upregulated in GC cells after exposure to 5-FU. This finding has not been reported in previous studies. Second, Overexpression of ITGA4 led to enhanced anti-apoptotic capacity and increased 5-FU resistance in GC. In addition, the functional role of ITGA4 in GC through the PI3K/AKT signaling pathway has also been further validated. Moreover, further exploration is warranted on whether ITGA4 inhibitors can serve as a synergistic treatment in combination with 5-FU for GC treatment. Meanwhile, whether ITGA4 can antagonize chemotherapeutic agents other than 5-FU, such as paclitaxel and oxaliplatin, remains to be further elucidated.

Data Sharing Statement

The data that supports the findings of this study, including any relevant details needed to reproduce the published results, are available from the corresponding author upon reasonable request.

Ethical Approval

According to point 1 of the 32 points of China's 2023 "Measures for Ethical Review of Life Science and Medical Research Involving Human Beings", research using legally available public data or non-intrusive observational data that does not harm individuals or involve sensitive personal or commercial information is exempt from ethical review. This study was based on publicly available databases, so there are no ethical issues or other conflicts of interest.

Acknowledgments

We thank PhD. Ning Wang (Huzhou Key Laboratory of Molecular Medicine, Huzhou Central Hospital, Fifth School of Clinical Medicine of Zhejiang Chinese Medical University, Huzhou, Zhejiang, 313000, People's Republic of China) for his kind assistance in revised correction.

Author Contributions

All authors made a significant contribution to the work reported, whether that is in the conception, study design, execution, acquisition of data, analysis and interpretation, or in all these areas; took part in drafting, revising or critically reviewing the article; gave final approval of the version to be published; have agreed on the journal to which the article has been submitted; and agree to be accountable for all aspects of the work.

Funding

This work was financially supported by the Zhejiang Province Public Welfare Technology Application Research Project (LGF20H16002) and Huzhou Municipal Science and Technology Bureau Project (2019GZB06).

Disclosure

The authors declare no conflict of interest in this work.

References

1. Sung H, Ferlay J, Siegel RL, et al. Global cancer statistics 2020: GLOBOCAN estimates of incidence and mortality worldwide for 36 cancers in 185 countries. *Ca a Cancer J Clinicians*. 2021;71(3):209–249. doi:10.3322/caac.2166
2. Smyth EC, Nilsson M, Grabsch HI, van Grieken NC, Lordick F. Gastric cancer. *Lancet*. 2020;396(10251):635–648. doi:10.1016/S0140-6736(20)31288-5
3. Dallas NA, Xia L, Fan F, et al. Chemoresistant colorectal cancer cells, the cancer stem cell phenotype, and increased sensitivity to insulin-like growth factor-i receptor inhibition. *Cancer Res*. 2009;69(5):1951–1957. doi:10.1158/0008-5472.CAN-08-2023
4. Rasmi Y, Nemati M, Pouya FD. Signaling pathways involved in 5-FU drug resistance in cancer. *Cancer Invest*. 2022;40(6):516–543. doi:10.1080/07357907.2022.2055050
5. Hashimoto Y, Yoshida Y, Yamada T, Aisu N, Hasegawa S. Current status of therapeutic drug monitoring of 5-fluorouracil prodrugs. *Anticancer Res*. 2020;40(8):4655–4661. doi:10.21873/anticanres.14464
6. Noa R, Michal T, Inbar P, et al. MalaCards: an amalgamated human disease compendium with diverse clinical and genetic annotation and structured search. *Nucleic Acids Res*. 2017;(D1):D877–D887. doi:10.1093/nar/gkw1012
7. Zdrazil B, Felix E, Hunter F, et al. The ChEMBL Database in 2023: a drug discovery platform spanning multiple bioactivity data types and time periods. *Nucleic Acids Res*. 2023;52(D1):D1180–D1192. doi:10.1093/nar/gkad1004

8. Damian S, Morris JH, Helen C, et al. The STRING database in 2017: quality-controlled protein–protein association networks, made broadly accessible. *Nucleic Acids Res*. 2017;45(D1):D362–D368. doi:10.1093/nar/gkw937
9. Magann AB, Grace MD, Rabitz HA, Sarovar M. Digital quantum simulation of molecular dynamics and control. *Phys Rev Res*. 2021;3(2). doi:10.1103/physrevresearch.3.023165
10. Brif C, Chakrabarti R, Rabitz HA. Control of quantum phenomena: past, present and future. *IOP Publishing*. 2010;(7). doi:10.1088/1367-2630/12/7/075008
11. Glaser SJ, Boscain U, Calarco T, et al. Training Schrödinger's cat: quantum optimal control. *Eur Phys J D*. 2015;69(12):279. doi:10.1140/epjd/e2015-60464-1
12. Keefer D, de Vivie-Riedle R. Pathways to new applications for quantum control. *Acc Chem Res*. 2018;51(9):2279–2286. doi:10.1021/acs.accounts.8b00244
13. Koch CP, Lemeshko M, Sugny D. Quantum control of molecular rotation. *Rev Mod Phys*. 2019;91(3):035005. doi:10.1103/revmodphys.91.035005
14. Abraham MJ, Murtola T, Schulz R, et al. GROMACS: high performance molecular simulations through multi-level parallelism from laptops to supercomputers. *SoftwareX*. 2015;1-2:19–25. doi:10.1016/j.softx.2015.06.001
15. Lu T, Chen F. Multiwfn: a multifunctional wavefunction analyzer. *J Comput Chem*. 2012;33(5):580–592. doi:10.1002/jcc.22885
16. Ueki S, Fujishima F, Kumagai T, et al. GR, Sgk1, and NDRG1 in esophageal squamous cell carcinoma: their correlation with therapeutic outcome of neoadjuvant chemotherapy. *BMC Cancer*. 2020;20(1):161. doi:10.1186/s12885-020-6652-7
17. Snider H, Villavarajan B, Peng Y, Shepherd LE, Robinson AC, Mueller CR. Region-specific glucocorticoid receptor promoter methylation has both positive and negative prognostic value in patients with estrogen receptor-positive breast cancer. *Clin Clin Epigenet*. 2019;11(1). doi:10.1186/s13148-019-0750-x
18. Liu CF, Shen QK, Li JJ, Tian YS, Quan Z. Synthesis and biological evaluation of novel 7-hydroxy-4-phenylchromen-2-one–linked to triazole moieties as potent cytotoxic agents. *J Enzyme Inhib Med Chem*. 2017;32(1):1111. doi:10.1080/14756366.2017.1344982
19. Qi Y, Qi W, Liu S, Sun L, Lv J. TSPAN9 suppresses the chemosensitivity of gastric cancer to 5-fluorouracil by promoting autophagy. *Cancer Cell Int*. 2020;20(1). doi:10.1186/s12935-019-1089-2
20. Lin X, Pan J, Hamoudi H, Yu J. THADA inhibits autophagy and increases 5-FU sensitivity in gastric cancer cells via the PI3K/AKT/mTOR signaling pathway. *Iran J Basic Med Sci*. 2024;27(2):195–202. doi:10.22038/IJBMS.2023.72055.15668
21. Young SA, McCabe KE, Bartakova A, et al. Integrin α4 enhances metastasis and may be associated with poor prognosis in MYCNlow neuroblastoma. *PLoS One*. 2015;10(5):e0120815. doi:10.1371/journal.pone.0120815
22. Klemke M, Weschenfelder T, Konstandin MH, Samstag Y. High affinity interaction of integrin α4β1 (VLA-4) and vascular cell adhesion molecule 1 (VCAM-1) enhances migration of human melanoma cells across activated endothelial cell layers. *J Cell Physiol*. 2007;212(2):368–374. doi:10.1002/jcp.21029
23. Zucchetto A, Vaisitti T, Benedetti D, et al. The CD49d/CD29 complex is physically and functionally associated with CD38 in B-cell chronic lymphocytic leukemia cells. *Leukemia*. 2012;26(6):1301–1312. doi:10.1038/leu.2011.369
24. Darzi L, Boshtam M, Shariati L, et al. The silencing effect of miR-30a on ITGA4 gene expression in vitro: an approach for gene therapy. *Res Pharm Sci*. 2017;12(6):456–464. doi:10.4103/1735-5362.217426
25. Lange KMD, Moutsianas L, Lee JC, Lamb CA, Barrett JC. Genome-wide association study implicates immune activation of multiple integrin genes in inflammatory bowel disease. *Nat Genet*. 2017;49(2):256–261. doi:10.1038/ng.3760
26. Xie J, Yang P, Lin HP, Li Y, Wang Z. Integrin α4 up-regulation activates the hedgehog pathway to promote arsenic and benzo[α]pyrene co-exposure -induced cancer stem cell-like property and tumorigenesis. *Cancer Lett*. 2020. doi:10.1016/j.canlet.2020.08.015
27. Pulkka OP, Mpindi JP, Tynninen O, et al. Clinical relevance of integrin alpha 4 in gastrointestinal stromal tumours. *J Cell & Mol Med*. 2018;22(4):2220–2230. doi:10.1111/jcmm.13502
28. Naren G, Guo J, Bai Q, Fan N, Nashun B. Reproductive and developmental toxicities of 5-fluorouracil in model organisms and humans. *Expert Rev Mol Med*. 2022;24:e9. doi:10.1017/erm.2022.3
29. He J, Zhang B, Zhou S, et al. Phase II study of perioperative camrelizumab and XELOX for locally advanced gastric or gastroesophageal junction adenocarcinoma. *Cancer Sci*. 2024. doi:10.1111/cas.16425
30. Yamaguchi K, Minashi K, Sakai D, et al. Phase IIb study of pembrolizumab combined with S-1 + oxaliplatin or S-1 + cisplatin as first-line chemotherapy for gastric cancer. *Cancer Sci*. 2022;113(8):2814–2827. doi:10.1111/cas.15462